Soil Environ. 45(2): xx-xx, 2026
DOI: doi.org/10.25252/SE/2026/254188
Online ISSN: 2075-1141
Print ISSN: 2074-9546

Spatial prediction of soil microvariability through chemometric modeling for precision agriculture

Sidique Kutubu[1,2], Ghulam Jilani[1], Muhammad Azeem[1*], Muhammad Naveed Tahir[3], Muhammad Iqbal[4] and Tajwar Alam[1]
[1]Institute of Soil & Environmental Sciences, PMAS Arid Agriculture University, Rawalpindi, Pakistan
[2]Kenema Forestry and Tree Crop Research Centre, Sierra Leone Agricultural Research Institute, Tower Hill, Freetown, Sierra Leone, West Africa
[3]Department of Agronomy, PMAS Arid Agriculture University, Rawalpindi, Pakistan
[4]Space & Upper Atmosphere Research Commission (SUPARCO), Islamabad, Pakistan
[Received:** May 10, 2026 **Accepted:** June 25, 2026 **Published Online:** July 13, 2026**]

Abstract

Conventional random sampling methods are inappropriate for comprehensive soil characterization and for generating high-resolution datasets. Therefore, microscale assessment of soil characteristics is imperative for monitoring soil conditions and implementing site-specific practices. The objectives of this study were to predict the physicochemical attributes of soil on a 50-hectare farm area by evaluating and categorizing spatial variability using geostatistical models and digital soil maps (DSM). The study area is at University Research Farm (URF), Koont, tehsil Gujar Khan, district Rawalpindi, Pakistan. It lies within the GPS coordinates of longitude from 73°0'45" E to 73°1'15" E and latitude from 33°6'45" N to 33°7'15" N. The farmland has sandy clay loam soil texture, and belongs to the Chakwal soil series and the Aridisols order of soil taxonomy. In the first phase of this study, 800 soil samples (0-15 cm deep) were collected from a 50-hectare farm area using a 25 m × 25 m grid defined by the Global Positioning System (GPS). In the second phase, a large dataset was acquired through wet-chemical analysis of soil properties, including the pH, EC, and contents of soil organic matter (SOM), NO_3-N, available-P, and extractable-K. During the third phase, spatial microvariability was assessed through descriptive statistics parameters (SD, CV, and skewness). Data showed greater differences among the soil samples for SOM, NO_3-N, and available-P contents, which were in the lower range. At the final stage, spatial interpolation was performed using semivariogram modeling and kriging to create the DSM. Chemometric analysis revealed that the best-fitted models were exponential for SOM, spherical for pH and EC, rational quadratic for NO_3-N, penta-spherical for P, and circular for K. Nugget-to-sill ratio (N/S) for SOM and K contents revealed strong spatial dependence; whereas, for pH, EC, NO_3-N, and available-P, it was moderate. The RMSE values < 1.0 for pH, EC, SOM, and NO3-N indicate the best-fit semivariogram models. In the DSM, most of the fields appeared normal with respect to pH and EC values. The SOM and NPK contents were displayed in the very low and medium ranges, covering >50 % of the total area. These findings establish that digital mapping is appropriate for assessing the soil properties in larger areas. In conclusion, the geostatistical modeling and DSM together facilitate soil characterization and prediction of soil attributes to categorize the large farm area into distinct soil management zones.

Keywords: Soil characteristics, Spatial variability, Geostatistical analysis, Semivariogram model, Kriging, Digital soil mapping

Introduction

Being the basis for agricultural development, the soil is an active natural body formed through pedogenic processes with variable chemical, physical, mineralogical, and biological properties along its depth to favor plant growth. The world's soil resources are facing unprecedented strain, with implications for regional and global food security in terms of both quantity and quality (FAO, 2025). About one-third of global agricultural land is classified as moderately to highly degraded, driven by several threats, including erosion,

***Email:** cmazeem@uaar.edu.pk
Cite This Paper: Kutubu, S., G. Jilani, M.Azeem, M.N. Tahir, M. Iqbal and T. Alam. 2026. Spatial prediction of soil microvariability through chemometric modeling for precision agriculture. *Soil and Environment*. doi.org/10.25252/SE/2026/254188.

compaction, salinization, low productivity, and loss of SOM (Smith *et al*., 2024). Declining soil productivity threatens food security; therefore, acquiring accurate, scientific, and multi-resolution soil data at the farm level is obligatory for sustainable land use planning and management (Abdu *et al.,* 2023). Field management through conventional practices has been designated among the basic causes of soil and crop variability. Traditionally practiced uniform nutrient application in the fields, regardless of the spatial variations, could waste the inputs and impair the soil and environment (Khan *et al.,* 2023). Precision agriculture technologies determine the variability in the field and use this information to meet crop needs more efficiently. Thus, agricultural productivity is intimately associated with soil attributes (Adeniyi *et al.,* 2024). Spatial soil information is crucial to decision-making on input management strategies for researchers as well as individual farmers (Piikki *et al.,* 2021). Understanding and assessment of the spatial variability in soil properties are imperative for evaluating the environment as they elucidate the factors and processes controlling the potential for crop production (Khan *et al.,* 2019b). Therefore, blanket recommendations for soil management that do not consider soil complexities and spatial variability are inappropriate for farmers' advisory services.

In non-systematic soil surveys, soil property boundaries are delineated from established maps of the surveyed areas. Broad field checks are constructed to determine the types of soil properties, but there is no internal assessment of soil variability. Therefore, larger-scale land maps are needed for micro-level planning and recommendations concerning soil fertility that could reduce fertilizer inputs without compromising the yield (Jalali, 2007). Continuous soil study offers a precise assessment of interior soil unevenness, which could enable farmers and stakeholders to manage their lands and optimize farm practices (Poccard-Chapuis *et al.,* 2021). Therefore, microscale assessments are crucial to evaluate soil productivity and crop performance. Geostatistics employs spatial interpolation techniques based on regionalized variables theory, which are more useful tools for describing the spatial variability of different soil attributes as compared to traditional statistical procedures (Oliver and Webster, 2015). Conventional soil mapping with labour-intensive field surveys and manual data collection procedures limits spatial coverage, resolution, and efficiency (Adeniyi *et al.,* 2024). Digital soil mapping (DSM) is a dynamic act of implementing management practices in accordance with the principles of precision agriculture (Filippi *et al*., 2024).

Soil microvariability assessment involves evaluating small-scale variations in soil properties and conditions within a specific area. This is important for understanding agricultural productivity, as large differences in soil characteristics may exist even over a small area. Thus, fertilizer application should be undertaken at variable rates as per the demand and availability of nutrients in each situation (Melo *et al.,* 2025). Soil microvariability assessment is undertaken mostly through grid sampling at regular intervals across the field in large numbers, conducting detailed analyses, employing geostatistical tools like variograms to examine variation with distance, and integrating the soil data with GIS to visualize soil characteristics across landscapes (Mondal *et al.,* 2022). Soil mapping for fertilizer prescriptions at variable rates is performed through regular grid sampling, which ensures uniform spatial coverage with a better representation of the entire field at regularly spaced intervals (Brus, 2019).

Soil characteristics inherently exhibit continuous spatial heterogeneity, and monitoring their dynamics across the farm area is impossible with routine/laborious soil sampling, analysis, and conventional statistical methods (Ahmed *et al.,* 2014). Chemometrics involving geostatistics uses stochastic interpretation tools based on regionalized random variables to obtain the best linear unbiased estimates of unsampled locations and elucidate the spatial variability of soil properties (Ziad *et al.,* 2016). Studies through GIS, GPS, and geostatistics indicate that soil variability ranges from a few millimeters to large fields encompassing numerous hectares (Khan *et al.,* 2019b). Combining the standard laboratory analyses with geostatistical models renders valuable information on the relationships among soil layer characteristics and their geomorphological units (Katzfuss, 2013). Digital soil mapping combines conventional soil survey procedures with modern computing approaches to predict soil properties. Precise spatial and spatio-temporal modeling via geostatistical procedures is important for the development of DSM and understanding spatial variations in soil characteristics (Adeniyi *et al.,* 2024). It considers the spatial and temporal variability of the soil characteristics depending on information related to ecological variables (Mosleh *et al.,* 2016). Such information is modeled for assessing the natural continuity of soil characteristics and to further demonstrate the gradual boundaries of different soils (Kopačková *et al.,* 2017).

Chemometrics involving geostatistical analysis via kriging incorporates spatial variability in the available dataset using the variogram model and generates the DSM (Khan *et al.,* 2023). Given the technical and socioeconomic constraints faced by farmers, the better approach is to develop soil maps for the whole farm rather than individual fields (Filippi *et al*., 2024). The present study aimed to evaluate the spatial variability and predict the physicochemical properties of soils across a 50-hectare farm area using geostatistical modeling and digital soil mapping with the GS+ software and ArcGIS geospatial platform.

Materials and Methods

Farm area and soil sampling

This study performed the detailed soil characterization of the University Research Farm (URF) near Koont village of the tehsil Gujar Khan in the district Rawalpindi of Pakistan. The URF belongs to PMAS Arid Agriculture University Rawalpindi, and is located 80 km from the university's main campus alongside the Mandra-Chakwal Road. Geographically, the URF is located between the GPS coordinate values of longitude from 73°0'45" E to 73°1'15" E, and latitude from 33°6'45" N to 33°7'15" N (Figure 1A, 1B), and at an altitude of 514 m above sea level (Naseem *et al.*, 2024). The URF has a total land area of about 100 hectares, with sandy clay loam soil texture, and belongs to the Chakwal soil series and the Aridisols order of soil taxonomy. It falls under the sub-humid and sub-tropical zones, with annual rainfall of 800-900 mm and mean daily temperatures ranging from 15-42ºC during summer and 4-25ºC in winter (Khan *et al.,* 2019a). Farm area experiences significant seasonal rainfall variations (Figure 1C), primarily driven by the wet summer monsoon during July-September (150-250 mm/month), followed by the mild spring rains in February-April (50-100 mm/month), with drier spans of pre-monsoon (May-June) and post-monsoon (October-December). The sampling points at the farm were marked through GPS coordinates using a grid size of 25 m × 25 m (Figure 1B). Soil samples were collected from 800 points over a 50-hectare area at a depth of 0-15 cm using a soil auger. Samples were preserved in plastic bags, labeled, transported to the laboratory, and prepared for analysis by standard procedures. These samples were first air-dried, ground, and screened through a 2 mm sieve. Then, the samples were subjected to analysis for the determination of various soil characteristics (pH, EC, SOM, N, P, and K contents). Data on these soil properties were processed using descriptive statistics and geostatistics procedures of semivariogram modeling and ordinary kriging. Spatial interpolation of the unsampled area was undertaken by creating the DSMs as spatial variability maps. Details of various steps in geostatistical modeling have been presented in Figure 2.

Soil analysis methods

The soil samples were analyzed for several soil characteristics, viz., pH, EC, and the contents of SOM, NO_3-N, available-P, and extractable-K. For measuring the pH and EC, soil suspensions were prepared using a 1:5 ratio of soil and distilled water. The suspensions were placed on a reciprocating shaker and allowed to mix thoroughly for 30 minutes, and then they were allowed to settle. The pH values were recorded using the glass electrode of a calibrated pH meter (McLean, 1982). The EC values of the same suspensions were measured through an EC meter after standardizing the conductivity meter with 0.01 *M* KCl solution (Paustian *et al.,* 1997). Contents of the SOM were assessed using the dichromate oxidation procedure (Walkley and Black, 1934). The NO_3-N was extracted in the AB-DTPA solution prepared from 1 M NH_4HCO_3 and 0.005 M DTPA, and its contents were determined using a spectrophotometer at a 540 nm wavelength (Soltanpour and Workman, 1979). Contents of available-P were extracted in a 0.5 M $NaHCO_3$ solution through shaking at 250 rpm and were determined using a spectrophotometer at the 882 nm wavelength (Recena *et al.,* 2017). The extractable-K was obtained in the 1 *N* ammonium acetate solution via shaking on a reciprocating shaker at 250 rpm. The contents of extractable-K were assessed on a flame photometer at the wavelength of 767 nm (Affinnih *et al.,* 2014).

Chemometric procedures

This study employed chemometric approaches, including mathematical, statistical, and geostatistical analyses, to evaluate soil properties. Descriptive statistical and geostatistical methods were adopted for semivariogram modeling and ordinary kriging to create DSMs from analytical data. The software packages used for processing the chemical analysis datasets of soil and extracting the required information were GS+ and ArcGIS geospatial platform. Details of these chemometric procedures of data analysis and spatial interpolation have been described hereunder, and displayed concisely in Figure 2.

Descriptive statistical analysis

Using the geostatistical software GS+ version 10 (Gamma Design Software, Plainwell, MI, USA), classical descriptive statistics were performed to obtain minimum, maximum, mean, standard deviation, coefficient of variation, kurtosis, and skewness values for soil properties, and to illustrate their distribution patterns (Glaz and Yeater, 2020). Spatial variability was assessed through the CV classification as <20, 20-50, and >50% corresponding to the low, moderate, and high variability in the data normalized by mean (Ameyan, 1986). Values of kurtosis in the range of -2 to +2 and of skewness in the range of -1 to +1 are adequate for normal variability in the data (Oliver and Webster, 2015).

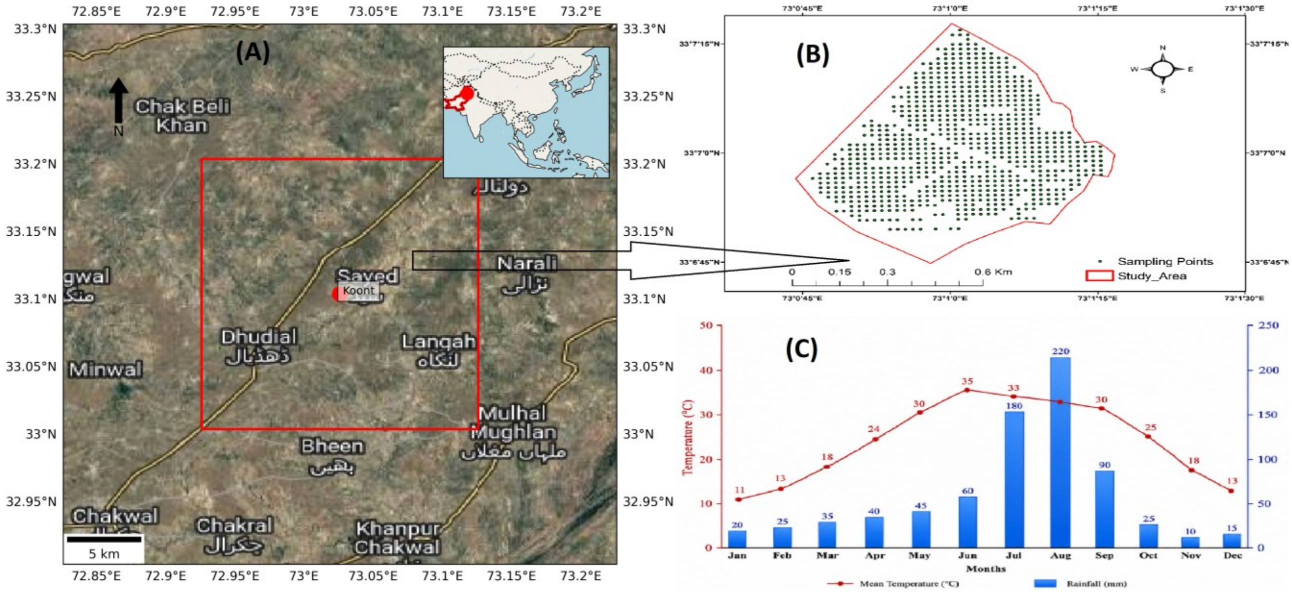

Figure 1: (A) Study area at URF, Koont, tehsil Gujar Khan of district Rawalpindi in Pakistan; (B) Soil sampling points at the study area; (C) Rainfall pattern at the study area

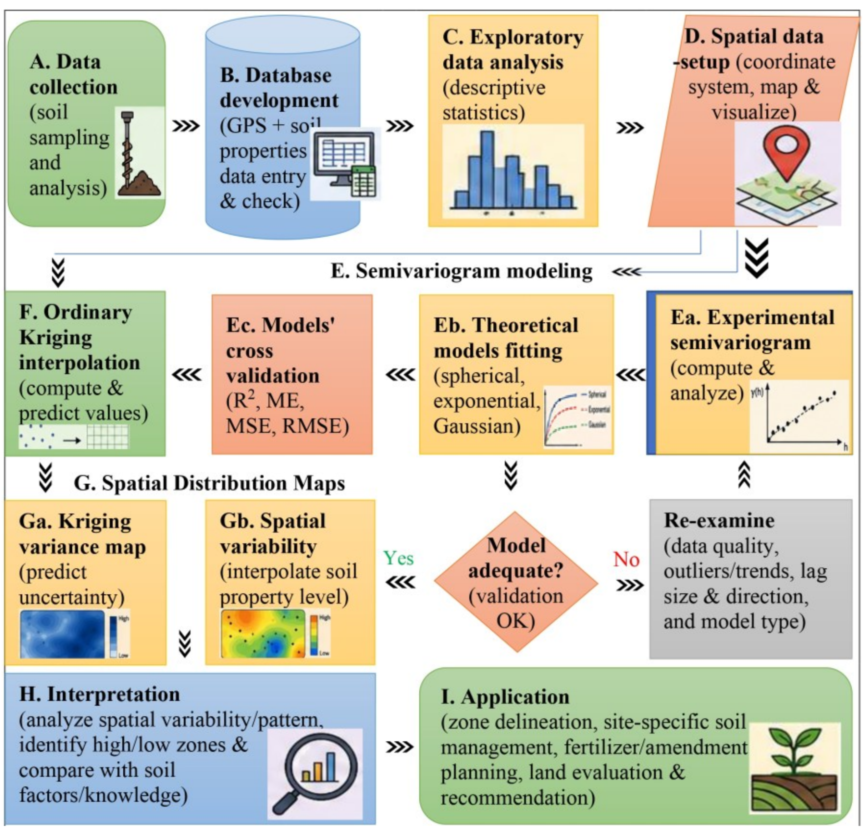

Figure 2: Different steps of spatial interpolation using semivariogram modeling and ordinary kriging procedure

Geospatial analysis and digital soil mapping

Geostatistical analysis employs spatial interpolation methods based on the regionalized variables theory, which are more useful tools for describing the spatial variability of different variables as compared to traditional statistical methods (Oliver and Webster, 2015). Semivariogram and kriging procedures of geostatistics are applied to predict and portray the spatial variability of soil characteristics in unobserved locations (Glaz and Yeater, 2020). Geostatistical procedures, including the construction of sample variograms and kriging, were performed through the GS+ software. Semivariograms were used to determine the degree of spatial dependence (autocorrelation in the data) for different variables (McBratney and Pringle, 1999). A semivariogram primarily comprises three basic parameters: viz., nugget, the local variance which occurs due to sampling error or measurement error; sill, the total variance; and range, the separation distance of spatial dependence between two sampling locations. Experimental semivariograms were fitted to different models (viz., exponential, spherical, penta-spherical, rational-quadratic, and circular) separately, and the best model was selected based on the fit (Yao *et al.,* 2019). The best one was designated for individual soil attributes on the basis of a lower RMSE value. Variogram model functionality (spatial dependence) in conjunction with ordinary kriging was employed to develop the prediction maps (Oliver and Webster, 2015).

Semivariance reflects the dispersion of all observations below the mean or target value of the data set (Aishah *et al.,* 2010). The nugget (N), sill (S), range, and N/S ratio parameters were derived from the semivariogram model to characterize the spatial distribution of soil attributes. Nugget is the small-scale variability or uncertainty due to local sampling error, sill is the total variance, range is the separation distance between the sampling points, and the N/S ratio characterizes the continuous spatial variation of each parameter correlating to its sampling points (Oliver and Webster, 2015). Nugget-to-sill ratio (N/S) measures the spatial dependence values (in percent) of soil attributes to classify them into high (< 25), medium (25-75), and low (> 75) categories of variability (Cambardella *et al*., 1994). Spatial dependence is also weak if the R^2 value falls below 0.50 (Liu *et al.,* 2008).

The ordinary kriging technique was employed for spatial interpolation and to produce the spatial variability maps of soil properties due to its greater flexibility. It estimates the value of a soil property at the unsampled locations using the structural property of a semivariogram. Several cross-validation indicators, viz., mean bias error (MBE), root mean square error (RMSE), average standard error (ASE), and root mean squared standardized error (RMSSE), were worked out to compare different models and to verify their accuracy of simulation (Robinson and Metternicht, 2006). The MBE or prediction mean error (PME) is the average of all errors in a set of measurements or forecasts, representing the average vertical distance between predicted values and actual values as positive or negative. It identifies bias in a model; an ideal value is "0", indicating no average bias. A negative MBE value (< 0) indicates underestimation (the model predicted values are lower than the actual/observed), while a positive MBE (> 0) indicates a tendency to overpredict. The ASE describes the average value of the standard error calculated for predictions. It is used to describe the average magnitude of standard errors of estimates across multiple parameters, or in specific modeling contexts (e.g., kriging in GIS), it represents the average of the standard errors calculated for predictions. The ASE value closer to RMSE is a prerequisite for accurate prediction (Hani *et al.,* 2010). The RMSE measures the average value of prediction error in a model as the average squared difference between predicted and observed values. It is the standard deviation of residuals (the differences between the observed and predicted values generated by a model) in the units of data, which may be of any value between zero and infinity (0 to +∞). The closer the metric is to "0", the better the model fits the data (though a perfect "0" is rarely achieved). Lower values indicate superior model performance, while higher values reflect poorer, less reliable predictions. Conversely, for the RMSSE, a value closer to "1" indicates the best-fitting semivariogram model for the interpolation map, yielding the most accurate prediction.

Interpolation maps of soil attributes were generated from the output of ordinary kriging and coordinates of sampling points through the geostatistical platform ArcGIS 11.1 (ESRI, Redlands, CA, USA). Leave-one-out cross-validation, along with different validation metrics, viz., MBE, RMSE, ASE, and RMSSE, was employed to select the best-fitted model (Piikki *et al.,* 2021). On this basis, the model having the RMSE value closer to ASE, the MBE/PME value closer to 0, and the RMSSE value closer to 1, is considered as the best fitting model for the interpolation map, giving the most accurate predictions (Laekemariam *et al.,* 2018; Abdu *et al.,* 2023).

Results

Explanatory statistical analysis

Descriptive statistical analysis of data on soil characteristics reveals that the range of values for each parameter reflected differently within the 50-hectare farm area (Table 1). The soil pH range (7.2-7.8) within the plot indicates a slightly alkaline status, with an average value of 7.7. The pH data show an exceptionally homogenous spatial distribution pattern across the study area. This is supported by a remarkably low absolute dispersion (SD = 0.2) and relative variability (CV = 2.2%), falling well below the 15% threshold typically used to denote low soil variability. However, the values of kurtosis (3.0) and skewness (1.2) for soil pH slightly exceed the thresholds for a perfectly normal distribution, which are between -2 and +2, and between -1 and +1, respectively. The EC is lower (1.4-2.3 dS m^{-1}) than the limit of saline conditions (> 4.0 dS m^{-1}), with an average value of 1.8 dS m^{-1}. Relative variation among the EC levels in statistical terms is low-to-moderate (SD 0.3, CV 16%), and follows a normal distribution pattern (kurtosis -0.5, skewness -0.4). It is highly typical for dynamic soil chemical properties influenced by minor micro-topographical variations and moisture gradients. In contrast to the highly uniform soil pH, both SOM and NO_3-N display extreme spatial heterogeneity across the study area. On average, both parameters fall into a depleted or 'low' fertility category, with mean values of 1.7% for SOM and 5.8 mg kg^{-1} for NO_3-N. Despite these low averages, their relative variability is exceptionally severe, yielding greater CV values of 73% and 82%, respectively. This extreme variability is highly characteristic of mobile and biologically active soil properties. While absolute measures like standard deviation (1.24% for OM; 4.76 mg kg^{-1} for NO_3-N) might superficially appear small, the CV normalizes these figures against their low means, exposing the true extent of the nutrient patchiness. Interestingly, despite this high variability, both properties conform well to an approximately normal distribution pattern, as evidenced by acceptable skewness (-0.4) and kurtosis (-0.5) values falling within the standard -1 to +1 threshold. The slightly negative, platykurtic nature of the distribution reflects a flat, broad spread of values across the fields rather than a centralized clustering, indicating distinct localized zones of nutrient accumulation and severe depletion.

Concentrations of available-P and extractable-K in the soil show their average value of 4.9 and 55 mg kg^{-1}, respectively, being in the medium ranges. Available-P concentration exhibits high variability (SD 3.5, CV 72 %) with a range of 2.4-16.5 mg kg^{-1} over the entire farm area. Extractable-K contents are in the range of 46-69 mg kg^{-1} with a low CV value of 11.3%. The kurtosis values for the soil properties except pH and SOM are within acceptable limits (between -2 and +2). Statistical evaluation of the data via skewness indicates that EC and extract-K fall in the range of normal distribution, being within the limits between -1 and +1. Other parameters show slightly lower or greater values than the normal range. The pH exceeds the normal distribution or variability limits of both kurtosis and skewness. The values of CV exhibit high variability among the samples for SOM, NO_3-N, and P, and show small variation for pH, EC, and K. Therefore, 800 soil samples drawn from a 50-hectare area are quite suitable, with sufficient ranges of variation to develop the DSM for predicting the aforementioned soil characteristics.

Interpolation with a kriging model (semivariogram)

The prediction accuracy of soil properties at unsampled locations was evaluated via kriging interpolation, using optimized parameters derived from the best-fit semi-variograms. Among the evaluated properties, extractable-K content exhibited noticeably higher RMSE/ASE values (23.9/22.3) compared to other parameters. This higher error estimate does not necessarily indicate a poor model fit; rather, it reflects the inherently high baseline concentration values and strong localized spatial variability characteristic of potassium in the 50-ha area. Data on semivariogram model parameters of interpolation by kriging for different soil

Table 1: Descriptive statistics of analytical data for physicochemical characteristics of soil samples from a 50-hectare farm area (n = 800)

Soil attributes	Min	Max	Mean	SD	CV (%)	Kurtosis	Skewness
pH	7.2	7.8	7.7	0.2	2.2	3.0	1.2
EC (dS m^{-1})	1.4	2.3	1.8	0.3	16	-0.5	-0.4
SOM (%)	0.2	3.3	1.7	1.6	73	2.2	-1.3
NO_3-N (mg kg^{-1})	1.1	10.5	5.8	4.7	82	1.5	-1.4
Avail-P (mg kg^{-1})	2.4	16.5	4.9	3.5	72	1.0	1.3
Extract-K (mg kg^{-1})	46	69	55	6.2	11	0.8	0.5

Abbreviations: n, number of samples; pH, negative logarithm of the hydrogen ion concentration; EC, electrical conductivity; SOM, soil organic matter; NO_3-N, nitrate-nitrogen; Avail-P, available phosphorus; Extract-K, extractable potassium; Min, minimum value; Max, maximum value; SD, standard deviation; CV, coefficient of variation.

characteristics have been presented in Table 2. Using these kriging functions for each soil property, the nugget-to-sill ratio (N/S, expressed as a percentage value) quantifies the strength of the autocorrelation and is displayed on the soil digital map. The N/S for SOM and K contents are below 25 %, indicating strong spatial dependence and well-correlated spatial data. Other parameters, viz., pH, EC, NO_3-N, and avail-P, exhibit slightly higher N/S ratios, which fall within the medium range (25-75%), indicating a moderate spatial dependence. The MBE values of all the soil attributes are slightly above "0" in the range of 0.001-0.138, reflecting that the models are accurate and fit, as the positive and negative errors have almost balanced out. The RMSE values of pH, EC, SOM, and NO_3-N are very close to the optimal value of "0", being < 1.0 to indicate the best fitted semivariogram models; avail-P has 1.64, while extract-K has a very high value of 23.9. The ASE values of all the soil characteristics have trends similar to those of RMSE values, with the same interpretation.

Nitrate-N contents in soil show a very low value of RMSE, which indicates that spatial correlation is very strong with lesser error. It also reflects that throughout the sampled

Table 2: Semivariogram model parameters of interpolation by kriging for different soil characteristics (n = 800)

Soil attributes	Model	N/S (%)	MBE	ASE	RMSE	RMSSE
pH	Spherical	27.2	0.003	0.12	0.15	1.00
EC	Spherical	27.5	0.003	0.19	0.21	1.06
SOM	Exponential	24.3	0.002	0.31	0.24	1.13
NO_3-N	Rational-quadratic	25.5	0.002	0.21	0.25	1.16
Avail-P	Penta-spherical	32.4	0.001	1.57	1.64	0.96
Extract-K	Circular	22.2	0.138	22.3	23.9	1.02

Abbreviations: n, number of soil samples; N/S, Nugget/Sill; MBE, mean bias error; ASE, average standardized error; RMSE, root mean square error; RMSSE, root mean square standardized error.

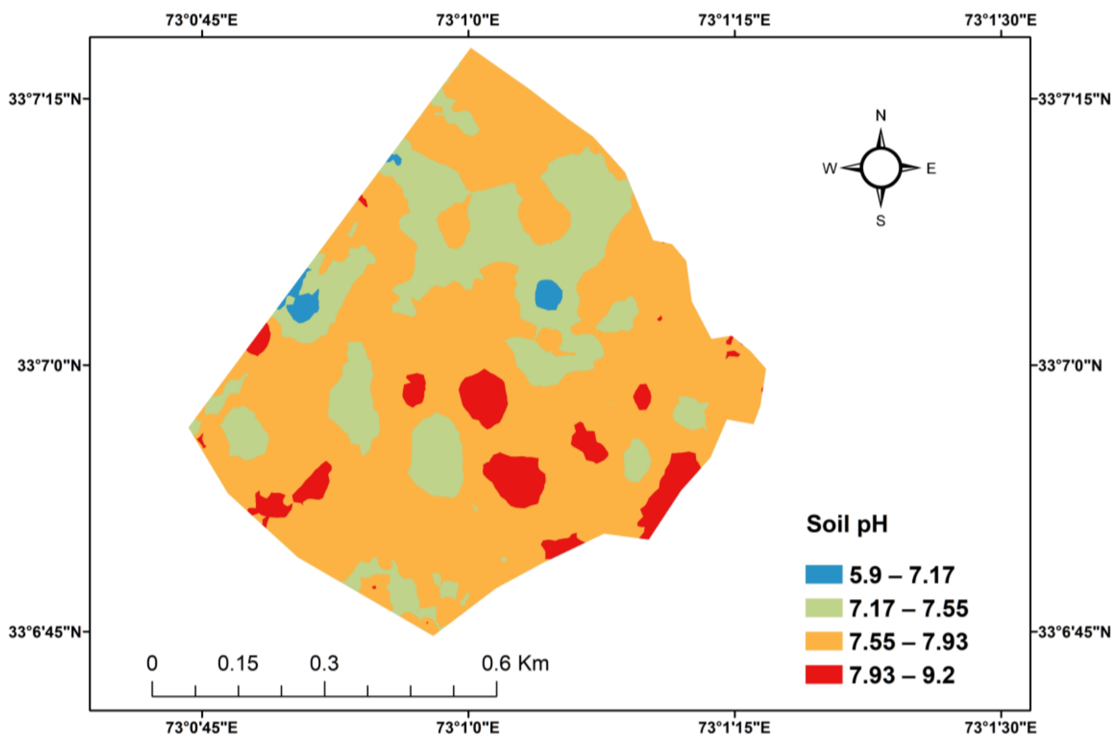

Figure 3: Digital soil map for the pH values at URF, Koont. Legends represent the range categories as: high (red), medium (orange), low (green), and very low (blue)

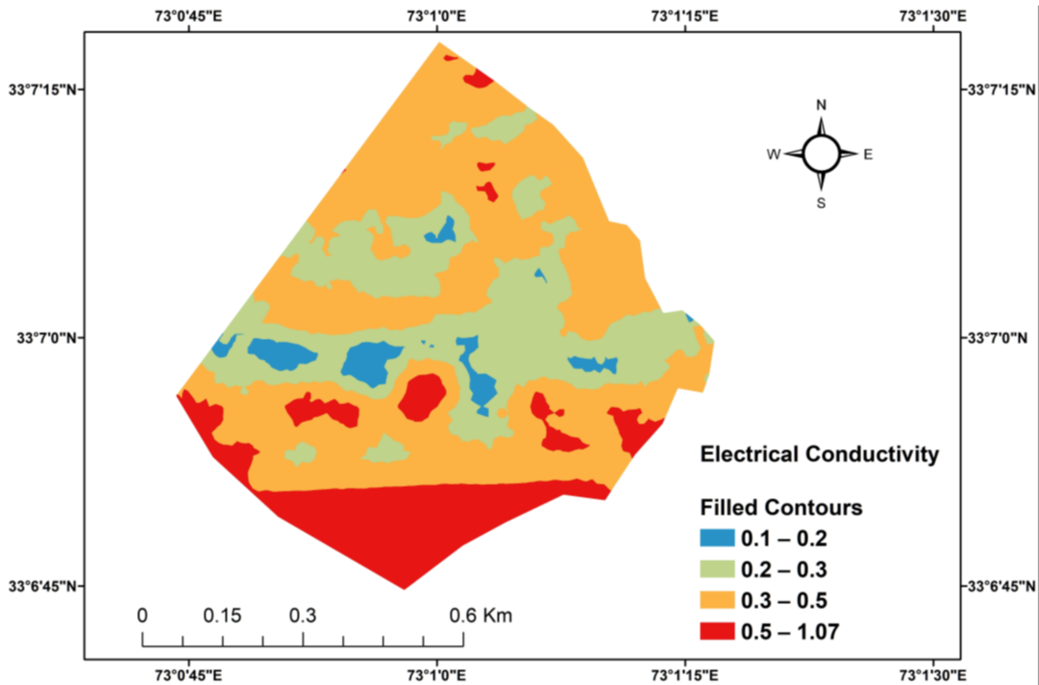

Figure 4: Digital soil map for the EC values at URF, Koont. Legends represent the range categories as: high (red), medium (orange), low (green), and very low (blue)

area (50-ha plot), the nitrogen contents are almost uniform with a small difference among samples. Similarly, the case is for soil pH and EC, which have the lowest values of RMSE, at 0.15 and 0.19, respectively. Phosphorus shows moderate error with a value of 1.64, which illustrates a strong autocorrelation within the plot. However, potassium depicts a high level of error with an RMSE value of 23.9, which shows that potassium is not evenly distributed within the farm area, and hence, the spatial correlation is weak. Similarly, the lower values of RMSSE being closer to "1" for all the soil attributes indicate good prediction by the semivariogram model. Therefore, they have been considered the best-fitting models for interpolation maps and to provide accurate predictions.

Digital Soil Maps of Soil Properties

The GIS-based DSM depicts the strength of autocorrelation of a particular soil property for the specific area, which has been sampled and analyzed. Soil sampling points evenly distributed over the 50-ha in the study area at URF, Koont, are shown in Figure 1 B. The sampled farm area spans from 73°0´45´´E to 73°1´15´´E and 33°6´45´´N to 33°7´15´´N coordinates. The range values of various soil characteristics have been shown in the legends, with red color indicating high values, medium values in orange, low in green, and very low values in blue color (Figures 3-8).

The DSM in Figure 3 portrays the spatial distribution of predicted pH values from the 50-ha field at URF, Koont. Most of the area appears with medium pH values (7.55-7.93), exhibiting a normal soil with no serious issues of acidity or alkalinity. Low-range pH (7.17-7.55) spans over 10-15% fields scattered throughout the farm. A few spots have very low (5.90-7.17) or high (7.93-9.20) pH values, which may hardly cover 5% of the total farm area. Figure 4 shows the strength of autocorrelation of the EC values in soil samples drawn from the farm area. The area distribution sequence of different EC categories may be described as: the medium range (0.3-0.5 dS m^{-1}) covers about 50% area, each of the high (0.50-1.07 dS m^{-1}) and low (0.2-0.3 dS m^{-1}) range expands over 20-25% area, and the very low EC range category (0.1-0.2 dS m^{-1}) covers 5-10% of the farm area. However, the DSM depicts that the whole farm area contains a concentration of salts lower than the critical salinity level of 4.0 dS m^{-1}. The SOM contents displayed in the DSM are shown in Figure 5. A major part falls under the medium (0.46-0.76%) and very low (0.061-0.36%) range of SOM, each covering about 40% of the total area. Whereas, each of the high (0.76-1.65%) and low (0.36-0.46%) categories spans over 5-10 % area.

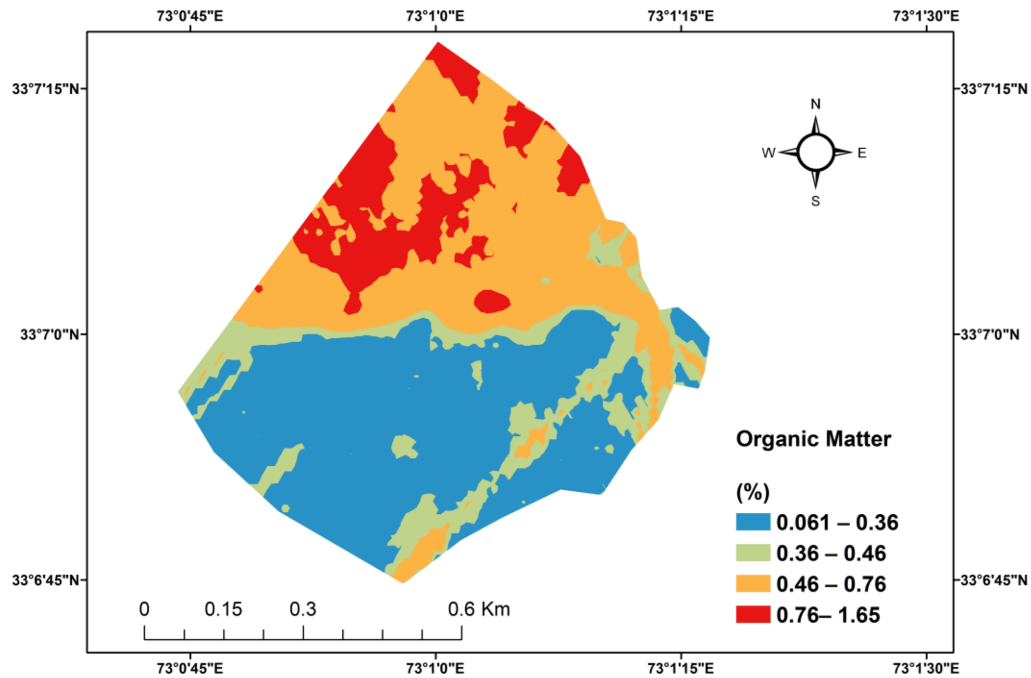

Figure 5: Digital soil map for the SOM content at URF, Koont. Legends represent the range categories as: high (red), medium (orange), low (green), and very low (blue)

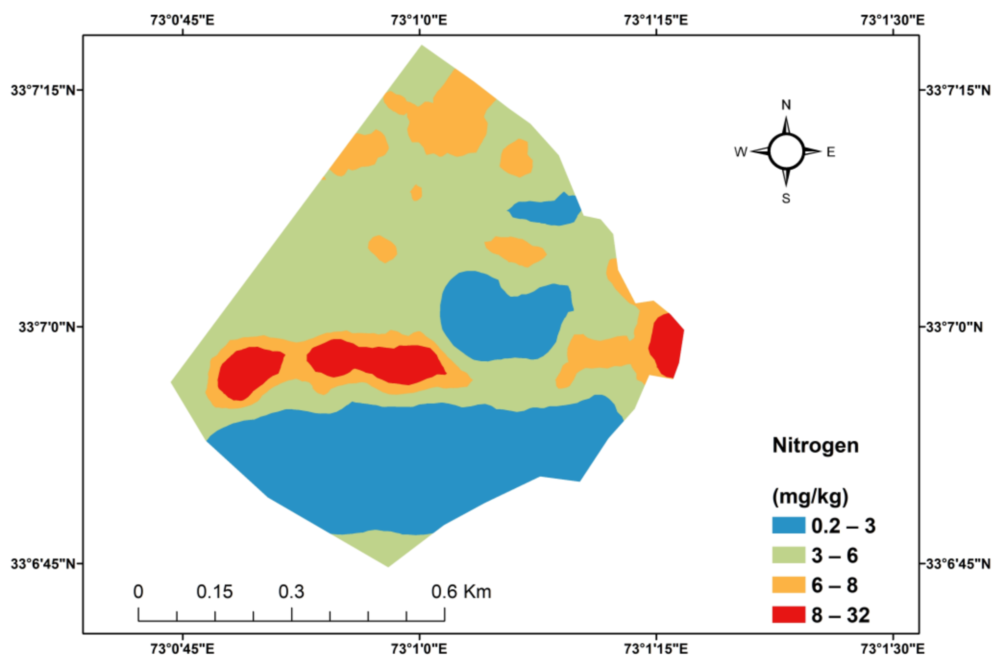

Figure 6: Digital soil map for the NO_3-N content at URF, Koont. Legends represent the range categories as: high (red), medium (orange), low (green), and very low (blue)

Figure 6 shows the DSM of NO_3-N content levels in the farm area. A large portion of the area (about 60%) has a low content (3-6 mg kg^{-1}), followed by the very low range of 0.2-3.0 mg kg^{-1} (around 30%). Each of the high (8-32 mg kg^{-1}) and medium (6-8 mg kg^{-1}) categories is scattered in a small area (about 5% of the total farmland). Concentration of the available-P in the soil samples has been displayed through DSM (Figure 7). The largest part of the farm area (about 70 %) falls under the medium P concentration in soil (3.72-7.17 mg kg^{-1}), followed by the high range of 7.17-61.71 mg kg^{-1} (about 20 %). Whereas, only about 8 % area shows the very low concentration of available-P (0.38-3.49 mg kg^{-1}), and low P content (3.49-3.72 mg kg^{-1}) is scattered in roughly 2% of the area. The DSM in Figure 8 illustrates the concentration of extractable-K in the soil samples. A large area (about 60 %) contains the medium range of potassium (50-85 mg kg^{-1}), followed by high (85-165 mg kg^{-1}) and low (25-50 mg kg^{-1}) categories of potassium in the soil (each in the range of 15-20 %). The very low concentration of extractable-K (3-25 mg kg^{-1}) spans over an area of about 5 % of the total.

Discussion

Descriptive statistics of various soil characteristics were used to illustrate their distribution patterns (Glaz and Yeater, 2020). Spatial microvariability was assessed through categorized values of CV (Ameyan, 1986), and kurtosis and skewness (Oliver and Webster, 2015). Analytical data obtained from the 50-ha farm area sampled with a grid size of 25 m × 25 m reflect that each parameter's values varied among the samples (Table I). The values of SD, CV, and skewness for SOM, NO_3-N, and available-P showed greater differences among the soil samples. A recent study at the same URF area by Naseem *et al*. (2024) reported its soil characteristics as: texture, sandy clay loam; SOM, 0.75 %; pH, 7.8; EC, 0.61 dS m^{-1}; NO_3-N, 3.74 mg kg^{-1}; available-P, 6.79 mg kg^{-1}; and extractable-K, 126 mg kg^{-1}. High variability in these soil properties may be due to the

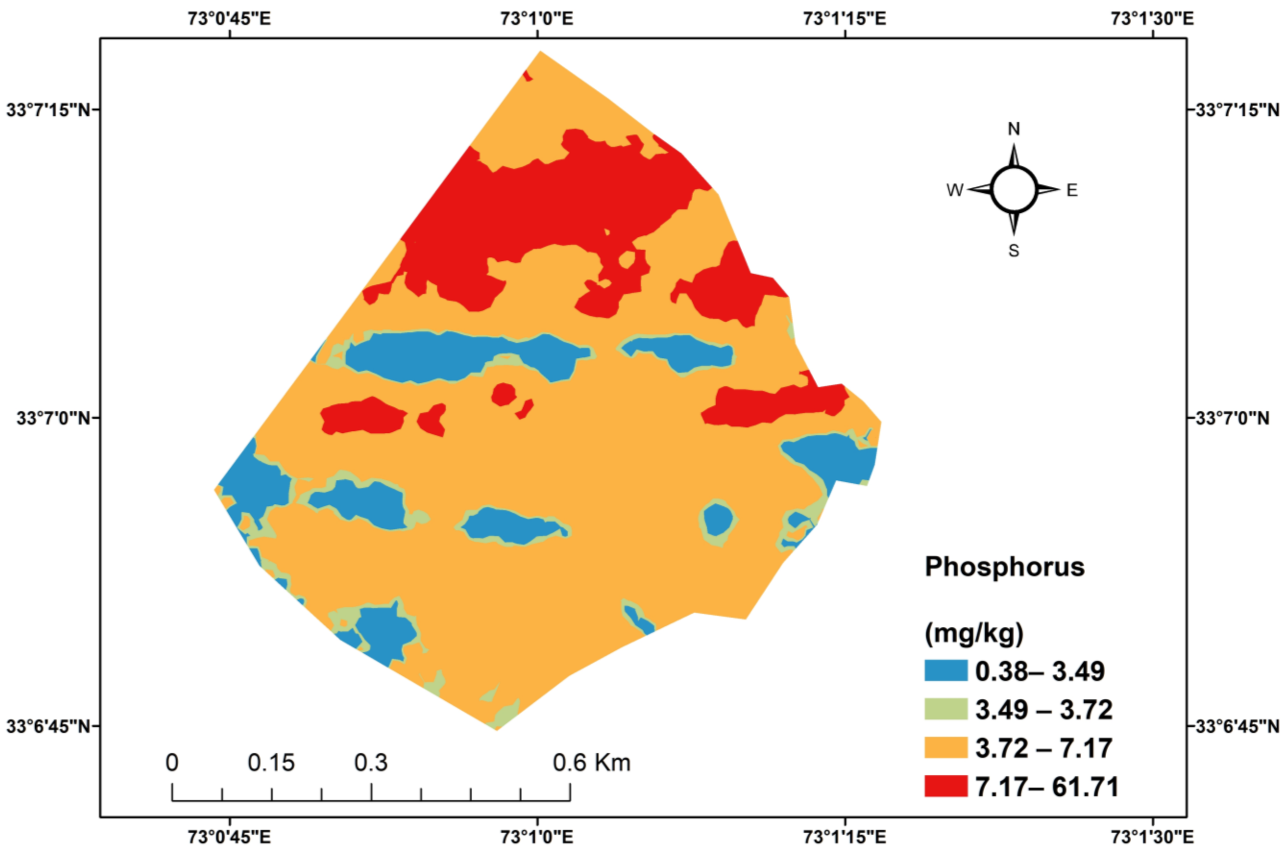

Figure 7: Digital soil map for the available-P content at URF, Koont. Legends represent the range categories as: high (red), medium (orange), low (green), and very low (blue)

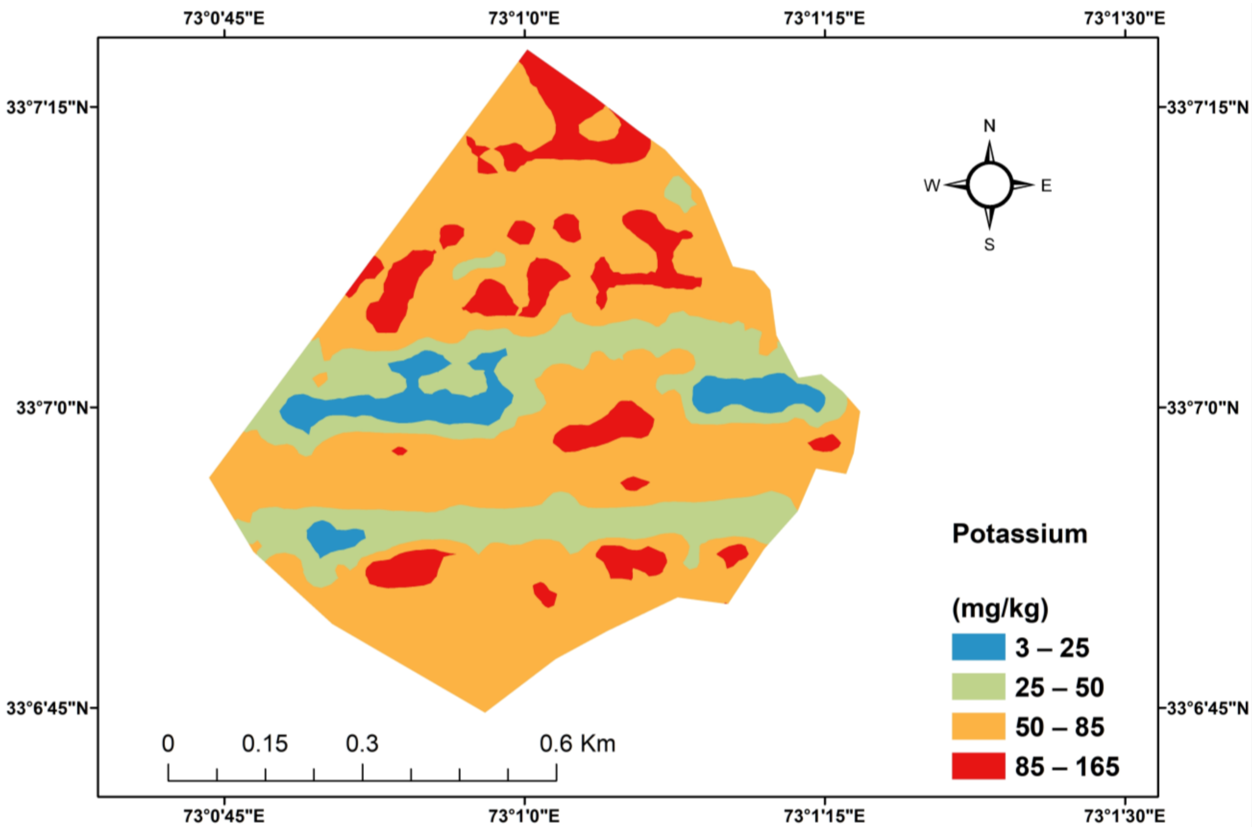

Figure 8: Digital soil map for the extractable-K content at URF, Koont. Legends represent the range categories as: high (red), medium (orange), low (green), and very low (blue)

cultivation of diverse crops across fields within the sampled farmland and to the variable application of N and P fertilizers to each crop. Further, farmlands are usually non-uniform, so soil variability is possible even in small areas (Melo *et al.,* 2025). The average contents of SOM, NO_3-N, and available-P are in the lower range. The majority of Pakistani soils have higher pH, low SOM, and are deficient in N, P, and micronutrient contents (Shakoor *et al.,* 2023). Organic matter has a direct relationship with nutrient availability in the soil (Joseph *et al.,* 2012). It emphasizes the need for microvariability assessment in agricultural fields to improve nutrient management. The low SOM content in intensively cultivated fields is associated with frequent tillage, increased mineralization, no use of organic amendments, and plant residue removal (Afzal *et al.,* 2024; Alfaris *et al.,* 2025). The pH, EC, and extractable-K content followed an approximately normal distribution as indicated by most statistical tests. Such soil attributes are largely controlled by inherent soil mineralogy and parent material and tend to remain relatively uniform across agricultural fields unless altered by external inputs such as fertilization or irrigation management (Adeniyi *et al*., 2024; Filippi *et al*., 2024). These findings emphasize the importance of assessing soil microvariability to improve resource allocation, enhance input efficiency, and support site-specific soil management strategies in precision agriculture systems (Khan *et al*., 2023).

Soil characteristics at unsampled sites have been assessed using kriging interpolation based on the best-fit semivariogram models (Table 2). Accordingly, the spherical model was used to interpolate soil pH and EC, exponential model for SOM, rational-quadratic for NO_3-N, penta-spherical for available-P, and circular model for extractable-K content. A suitable model is selected by using the interpolation parameters of ME, MSE, RMSE, ASE, and RMSSE (Arétouyap *et al.,* 2016). The N/S ratio for SOM and K contents (< 25 %) reflected strong spatial dependence and well-correlated spatial data. Both organic matter and potassium are present in soil inherently, as well as added to improve soil productivity. Also, they are relatively immobile in the soil profile once incorporated due to stable humic substances of SOM and K-fixation in clay minerals.

Therefore, their contents vary spatially and with the soil amendment practices. Whereas, pH, EC, NO_3-N, and available-P are within the medium range of N/S (25-75%), showing a moderate spatial dependence. Spatial variability of several soil properties depends on intrinsic factors, like parent material and texture, as well as extrinsic factors, e.g., fertilizer type/dose, and irrigation, etc. (Sun *et al.,* 2022). The MBE values of the tested soil properties are close to "0", indicating that the models are accurate and best-fit. It indicates the average prediction error, and values around zero neither reflect systematic overestimation nor underestimation (Fairbairn *et al.,* 2024). Usually, MBE is paired with RMSE to ascertain the accuracy and precision of the model. The RMSE values of pH, EC, SOM, and NO_3-N are <1.0, reflecting the best-fit semivariogram models; available-P has 1.64, while extractable-K has a very high value of 23.9. In a study with a 20-m sampling interval, total N, available P, and available K showed the lowest interpolation errors (Liu *et al.,* 2010). Soil pH, EC, and NO_3-N content with lower RMSE values reflect that these characteristics are almost uniform throughout the 50-ha sampled area. Phosphorus has a moderate RMSE value, reflecting a strong autocorrelation within the plot. However, potassium shows a very high RMSE, indicating weak spatial correlation and uneven distribution within the sampled area. Higher RMSE values for P and K contents could be due to the difference in their fertilizer input to various crops grown in different fields. Zhang *et al.* (2014) studied the spatial variability of soil nutrients and found that N, P, K, and pH were moderately spatially dependent. For the sake of cross-validation, the ASE values were tabulated and found similar to RMSE, which obviously had the same interpretation. If these values are similar in kriging, it indicates that the model is well-calibrated and produces reliable uncertainty estimates (Arétouyap *et al.,* 2016). As an indicator of a well-fitted model, validation requires ASE values near RMSE, which reflects that predicted errors are consistent with actual errors (Hani *et al.,* 2010).

The DSM portrayed in Figures 2-7 revealed various soil attributes over a 50-ha field at URF, Koont. Most of the fields (about 80 %) throughout the farm area appear with pH values between 7.55 and 7.93, which indicates a normal soil with no serious issue of acidity or alkalinity. It is in line with the fact that the majority of Pakistani cultivated soils are slightly alkaline due to their calcareous origin (Ullah *et al.,* 2025). The distribution sequence of different EC categories indicates that the medium range covers about 50 % area, and each of the high and low ranges expands over 20-25% of the farm area. Yet, the DSM reflects that the entire farm area contains salt concentration lower than the critical salinity level of 4.0 dS m^{-1}. Over the 79.61 million hectares of the total geographic area of Pakistan, a range from 4.50 to 6.67 million hectares of salt-affected soils (nearly 40,000 hectares becoming saline annually) represents 25-30% of Pakistan's 22 million hectares of agricultural land (Syed *et al.,* 2021). The lower content of salts in the soil at Koont farm could be attributed to its sub-humid and subtropical climate and mild slope, with annual rainfall of 800-900 mm, which facilitates the surface-wash and leaching of salts (Shaheen, 2016; Idrees *et al.,* 2022). The SOM content displayed in the DSM reflects that a major proportion falls within the very low and medium range, each covering about 40% of the total area. The SOM frequency distribution analysis in the Gujar Khan and Fatehjang tehsils of Rawalpindi in the Pothwar region indicated that most of the soils were deficient in SOM, and 45% soils of Gujar Khan had OM content in the medium range of 0.4-0.6% (Shaheen *et al,* 2008; Rehman *et al.,* 2021). The content of NO_3-N in the major portion of the area (about 60%) has been categorized as low, followed by the very low range (about 30%). Available-P and extractable-K on the largest part of the farm area (60-70%) fall under the medium concentration, followed by the high range (15-20 %). In the Gujar Khan tehsil of the Pothohar plateau, a major proportion of soils fall within the low to medium fertility range with respect to NPK (Rehman *et al.,* 2021; Iqbal *et al.,* 2022). The relatively low NO_3-N contents observed in the soils of the Pothwar region have been associated with runoff losses, leaching, and the imbalanced application of nitrogen fertilizers under rainfed conditions (Shaheen, 2016; Ahmed *et al.,* 2023). It has also been reported that phosphorus availability is frequently limited due to fixation by calcium carbonate in calcareous soils and its removal through erosion-associated sediment transport in sloping landscapes (Khan *et al.,* 2020; Ali *et al.,* 2024). Soils of Pakistan, particularly in the Pothohar region, are generally rich in mica-bearing minerals, which serve as a natural source of potassium; therefore, potassium deficiency is comparatively less severe, with many soils showing medium K status in Gujar Khan and surrounding areas (Rehman *et al.,* 2021; Hussain *et al.,* 2023). In a broader context, the soil characteristics revealed through digital soil mapping (DSM) in the present study are consistent with previous findings reported for this region, confirming the reliability of spatial variability-based soil assessment approaches (Iqbal *et al.,* 2022).

Conclusions

The principal emphasis of this case study was to develop geostatistical predictive models for microvariability assessment of soil attributes by creating DSMs for a 50-hectare area at URF, Koont, Gujar Khan tehsil of Rawalpindi district in Pakistan. Using a grid size of 25 m × 25 m, 800 samples were drawn and analyzed for various soil characteristics. Geostatistical analysis was performed to incorporate spatial microvariability into the available dataset, using semivariogram models and ordinary kriging to generate the DSM. Through chemometric and geostatistical kriging analysis, the study applied specific best-fit semivariogram models such as spherical for pH and EC, and exponential for soil organic matter (SOM) validated by low mean error and root-mean-square error metrics. The resulting maps and descriptive statistics revealed that while pH, EC, and extractable-K were relatively uniform and normally distributed, attributes like SOM, NO_3-N, and available-P exhibited high variability and predominantly lower-range averages across the farm. These distribution patterns align with historical regional data and demonstrate that integrating legacy databases with chemometric DSM modeling provides a highly accurate, site-specific framework to help farmers optimize nutrient management and resource allocation.

References

Abdu, A., F. Laekemariam, G. Gidago, A. Kebede and L. Getaneh. 2023. Variability analysis of soil properties, mapping, and crop test responses in Southern Ethiopia. *Heliyon* 9(3): 14013.

Adeniyi, O.D., H. Bature and M. Mearker. 2024. A systematic review on digital soil mapping approaches in lowland areas. *Land* 13(3): 379.

Affinnih, K., I. Salawu and A. Isah. 2014. Methods of available potassium assessment in selected soils of Kwara State, Nigeria. *Agrosearch* 14(1): 76-87.

Afzal, T., A. Wakeel, S.A. Cheema, J. Iqbal and M. Sanaullah. 2024. Influence of quality and quantity of crop residues on organic carbon dynamics and microbial activity in soil. *Soil & Environment* 43(1): 53-64.

Ahmed, H., M.T. Siddique, S. Ali, N.A. Abbasi, A. Khalid and R. Khalid. 2014. Micronutrient indexing in the apple orchards of Northern Punjab, Pakistan using geostatistics and GIS as diagnostic tools. *Soil & Environment* 33(1): 7-16.

Ahmed, M., A. Ali, R. Khalid and S. Ahmad. 2023. Nutrient losses and nitrogen dynamics in rainfed agro-ecosystems of Pothohar Plateau, Pakistan. *Pakistan Journal of Agricultural Sciences* 60(2): 215-226.

Aishah, A.W., S. Zauyah, A.R. Anuar and C.I. Fauziah. 2010. Spatial variability of selected chemical characteristics of paddy soils in Sawah Sempadan, Selangor, Malaysia. *Malaysian Journal of Soil Science* 14: 27-39.

Alfaris, M., M. Ramadhan and A.S. Al-Bayati. 2025. Evaluation of the effects of deep tillage and organic amendments on soil characteristics and sunflower and okra yield across successive seasons. *Soil & Environment* 44(2): 168-176.

Ali, M.A., A. Khan, S.M.A. Shah and A. Rehman. 2024. Phosphorus dynamics and fixation in calcareous soils of semi-arid regions of Pakistan. *Journal of Soil Science and Plant Nutrition* 24(1): 98-112.

Ameyan, O. 1986. Surface soil variability of a map unit on Niger River alluvium. *Soil Science Society of America Journal* 50(5): 1289-1293.

Arétouyap, Z., P. Njandjock Nouck, R. Nouayou, F.E. Ghomsi Kemgang, A.D. Piépi Toko and J. Asfahani. 2016. Lessening the adverse effect of the semivariogram model selection on an interpolative survey using kriging technique. *SpringerPlus* 5(1): 549.

Brus, D.J. 2019. Sampling for digital soil mapping: A tutorial supported by R scripts. *Geoderma* 338: 464-480.

Cambardella, C.A., T.B. Moorman, J.M. Novak, T.B. Parkin, D.L. Karlen, R.F. Turco and A.E. Konopka. 1994. Field-scale variability of soil properties in Central Iowa soils. *Soil Science Society of America Journal* 58: 1501-1511.

Fairbairn, D., P. de Rosnay and P. Weston. 2024. Evaluation of an adaptive soil moisture bias correction approach in the ECMWF land data assimilation system. *Remote Sensing* 16(3): 493.

FAO. 2025. The State of the World's Land and Water Resources for Food and Agriculture 2025 - The potential to produce more and better. Food and Agriculture Organization of the United Nations, Rome, Italy. 148 p.

Filippi, P., B.M. Whelan and T.F.A. Bishop. 2024. Proximal and remote sensing – what makes the best farm digital soil maps? *Soil Research* 62: 23112.

Glaz, B. and K.M. Yeater. 2020. Applied Statistics in Agricultural, Biological, and Environmental Sciences. John Wiley & Sons Ltd., Hoboken, New Jersey. 672 p.

Hani, A., E. Pazira, M. Manshouri, K.S. Babaie and M.T. Ghahroudi. 2010. Spatial distribution and mapping of risk elements pollution in agricultural soils of southern Tehran, Iran. *Plant, Soil and Environment* 56: 288-296.

Hussain, S., J. Iqbal, M. Farooq and T. Abbas. 2023. Potassium availability and mineralogical controls in soils of Pothohar Plateau, Pakistan. *Soil & Environment* 42(1): 45-56.

Idrees, M., S. Ahmad, M.W. Khan, Z.H. Dahri, K. Ahmad, M. Azmat and I.A. Rana. 2022. Estimation of water balance for anticipated land use in the Potohar Plateau of the Indus Basin using SWAT. *Remote Sensing* 14: 5421.

Iqbal, M., S. Khan, H. Rehman and A. Tariq. 2022. Soil fertility status and spatial variability assessment using geostatistics in Gujar Khan, Pakistan. *Journal of Integrative Agriculture* 21(8): 2305-2317.

Jalali, M. 2007. Spatial variability in potassium release among calcareous soils of western Iran. *Geoderma* 140: 42-51.

Joseph, M.M., K.R. Renjith, C.S. Ratheesh Kumar and N. Chandramohanakumar. 2012. Assessment of organic matter sources in the tropical mangrove ecosystems of Cochin, Southwest India. *Environmental Forensics* 13(3): 262-271.

Katzfuss, M. 2013. Bayesian nonstationary spatial modeling for very large datasets. *Environmetrics* 24: 189-200.

Khan, A., M. Rafiq, Ali, F. and Shah, Z. 2020. Soil erosion and nutrient transport processes in sloping agricultural lands of northern Pakistan. *Environmental Monitoring and Assessment* 192: 642.

Khan, A.A., M.I. Ashraf, S.U. Malik, S. Gulzar and M. Amin. 2019a. Spatial trends in surface runoff and influence of climatic and physiographic factors: A case study of watershed areas of Rawalpindi district. *Soil & Environment* 38(2): 181-191.

Khan, M.Z., M.A. Islam, M.S. Amin and M.M.R. Bhuiyan. 2019b. Spatial variability and geostatistical analysis of selected soil properties. *Bangladesh Journal of Scientific and Industrial Research* 54(1): 55-66.

Khan, H., T.J. Esau, A.A. Farooque, Q.U. Zaman, F. Abbas and A.W. Schumann. 2023. Soil spatial variability and its management with precision agriculture. p. 19-36. *In:* Precision Agriculture: Evolution, Insights and Emerging Trends. Elsevier Inc., Amsterdam, Netherlands.

Kopačková, V., A. Rúfusová and K. Novotná. 2017. Gradual boundaries of soil units and their impact on soil mapping. *Acta Universitatis Agriculturae et Silviculturae Mendelianae Brunensis* 65(2): 471-481.

Laekemariam, F., K. Kibret, T. Mamo and H. Shiferaw. 2018. Accounting spatial variability of soil properties and mapping fertilizer types using geostatistics in southern Ethiopia. *Communications in Soil Science and Plant Analysis* 49: 124-137.

Liu, G.-S., H.-L. Jiang, S.-D. Liu, X.-Z. Wang, H.-Z. Shi, Y.-F. Yang, X.-M. Yang, H.-C. Hu, Q.-H. Liu and J.-G. Gu. 2010. Comparison of kriging interpolation precision with different soil sampling intervals for precision agriculture. *Soil Science* 175(8): 405-415.

Liu, X., K. Zhao, J. Xu, M. Zhang, B. Si and F. Wang. 2008. Spatial variability of soil organic matter and nutrients in paddy fields at various scales in South China. *Environmental Geology* 53: 1139-1147.

McBratney, A.B. and M.J. Pringle. 1999. Estimating average and proportional variograms of soil properties and their potential use in precision agriculture. *Precision Agriculture* 1(2): 125-152.

Mclean, E.O. 1982. Soil pH and lime requirement. p. 199-224. In: A.L. Page (ed.), Methods of Soil Analysis. Part 2. Chemical and Microbiological Properties. Soil Science Society of America, Madison.

Melo, D.D., I.A. Cunha and L.R. Amaral. 2025. Hierarchical stratification for spatial sampling and digital mapping of soil attributes. *AgriEngineering* 7(1): 10.

Mondal, B.P., R.N. Sahoo, K.K. Bandyopadhyay, B. Das, A. Arora and J. Mukherjee. 2022. Assessment of spatial variability of soil available sulphur using geostatistical techniques in a part of Deccan Plateau of India. *Journal of the Indian Society of Soil Science* 70(2): 237-242.

Mosleh, Z., M.H. Salehi, A. Jafari, I.E. Borujeni and A. Mehnatkesh. 2016. The effectiveness of digital soil mapping to predict soil properties over low-relief areas. *Environmental Monitoring and Assessment* 188: 1-13.

Naseem, M., A.N. Chaudhry, G. Jilani, F. Naz, T. Alam and D.M. Zhang. 2024. Biosynthesis and characterization of extracellular polymeric substances from divergent microbial and ecological bioresources. *Arabian Journal for Science and Engineering* 49(7): 9043-9052.

Oliver, M.A. and R. Webster. 2015. Basic Steps in Geostatistics: The Variogram and Kriging. Springer International Publishing, Cham, Switzerland. 100 p.

Paustian, K., O. Andren, H.H. Janzen, R. Lal, P. Smith, G. Tian, H. Tiessen, M. van Noordwijk and P.L. Woomer. 1997. Agricultural soils as a sink to mitigate CO_2 emissions. *Soil Use and Management* 13: 230-244.

Piikki, K., J. Wetterlind, M. Söderström and B. Stenberg. 2021. Perspectives on validation in digital soil mapping of continuous attributes: A review. *Soil Use and Management* 37: 7-21.

Poccard-Chapuis, R., S. Plassin, R. Osis, D. Pinillos, G. Martinez Pimentel, M.C. Thalês, F. Laurent, M.R. de Oliveira Gomes, L.A. Ferreira Darnet, J. de Carvalho Peçanha and M.G. Piketty. 2021. Mapping land suitability to guide landscape restoration in the Amazon. *Land* 10(4): 368.

Recena, R., I. Díaz and A. Delgado. 2017. Estimation of total plant available phosphorus in representative soils from Mediterranean areas. *Geoderma* 297: 10-18.

Rehman, O.U., S.M. Mehdi, R. Abad, S. Saleem, R. Khalid, S.T. Alvi and A. Munir. 2021. Soil characteristics and fertility indexation in Gujar Khan area of Rawalpindi. *Pakistan Journal of Scientific & Industrial Research Series A: Physical Sciences* 64(1): 46-51.

Robinson, T.P. and G. Metternicht. 2006. Testing the performance of spatial interpolation techniques for mapping soil properties. *Computers and Electronics in Agriculture* 50: 97-108.

Shaheen, A., M. Shafiq, M.A. Naeem and G. Jilani. 2008. Soil characteristics and plant nutrient status in the eroded lands of Fatehjang in the Pothwar Plateau of Pakistan. *Soil & Environment* 27(2): 208-214.

Shaheen, A. 2016. Characterization of eroded lands of Pothwar Plateau, Punjab, Pakistan. *Sarhad Journal of Agriculture* 32(3): 192-201.

Shakoor, A., G. Jilani, T. Iqbal, I. Mahmood, T. Alam, M.A. Ali, S.S.H. Shah and R. Ahmad. 2023. Synthesis of elemental- and nano-sulfur-enriched bio-organic phosphate composites, and their impact on nutrients bioavailability and maize growth. *Journal of Soil Science and Plant Nutrition* 23(3): 3281-3289.

Smith, P., R.M. Poch, D.A. Lobb, R. Bhattacharyya, G. Alloush, G.D. Eudoxie, L.H. Anjos, M. Castellano, G.M. Ndzana, C. Chenu, R. Naidu, J. Vijayanathan, A.M. Muscolo, G.A. Studdert, N.R. Eugenio, M.C. Calzolari, N. Amuri and P. Hallett. 2024. Status of the World's Soils. *Annual Review of Environment and Resources* 49(1): 73-104.

Soltanpour, P.N. and S. Workman. 1979. Modification of the NH_4HCO_3-DTPA soil test to omit carbon black. *Communications in Soil Science and Plant Analysis* 10(11): 1411-1420.

Sun, G., H. Liu, D. Cui and C. Chai. 2022. Spatial heterogeneity of soil nutrients in Yili River Valley. *PeerJ* 10: e13311.

Syed, A., G. Sarwar, S.H. Shah and S. Muhammad. 2021. Soil salinity research in 21st century in Pakistan: Its impact on availability of plant nutrients, growth and yield of crops. *Communications in Soil Science and Plant Analysis* 52(3): 183-200.

Ullah, R., K. Sahar, S.W. Qamar and S. Saqib. 2025. Analysis of soil physicochemical parameters in the Thal desert ecosystem: A case study from Kallur Kot, Indus River eastern bank. *International Journal of Advances in Sustainable Development* 2(2): 19-31.

Walkley, A. and I.A. Black. 1934. An examination of the Degtjareff method for determining soil organic matter, and a proposed modification of the chromic acid titration method. *Soil Science* 37(1): 29-38.

Yao, X., K. Yu, Y. Deng, Z. Qi, Z. Lai and J. Liua. 2019. Spatial distribution of soil organic carbon stocks in Masson pine forests in subtropical China. *Catena* 178: 189-198.

Zhang, Z., B. Hu and G. Hu. 2014. Spatial heterogeneity of soil chemical properties in a subtropical karst forest, Southwest China. *The Scientific World Journal* 2014: 473651.

Ziad, T., M.T. Siddique, K.S. Khan, N.A. Abbasi and H.A.M. Iqbal. 2016. Indexing bioavailable and foliage boron content in apple orchards of Pishin district, Baluchistan, using GIS and geo-statistics as diagnostic tools. *Soil & Environment* 35(1): 35-45.